Theoretical study of the effect of the solvent on the electronic properties of pyrimidopyrimidine derivatives

Tayeb Chieb, Abdelkader Ladjarafi, Billel Teyar, Jean-François Halet

Theoretical study of the effect of the solvent on the electronic properties of pyrimidopyrimidine derivatives

Tayeb Chieb[a], Abdelkader Ladjarafi[b,c,*], Billel Teyar[b,d], Jean-François Halet[e,*]

[a] *Department of Biology, Faculty of Natural and Life Sciences, University Ziane Achour, UZAD, 17003, Djelfa, Algeria*
[b] *Laboratory of Physico-chemistry of Materials and Environment, Faculty of Exact Sciences and Computer Sciences, University Ziane Achour, UZAD, 17003, Djelfa, Algeria*
[c] *Laboratory of Thermodynamics and Molecular Modelling, Faculty of Chemistry, USTHB, 17003, Algiers, Algeria*
[d] *URCHEMS, Department of Chemistry, Mentouri Brothers University, 25017, Constantine, Algeria*
[e] *CNRS – Saint-Gobain – NIMS, IRL 3629, Laboratory for Innovative Key Materials and Structures (LINK), National Institute for Materials Science (NIMS), Tsukuba, 305-0044, Japan*

* Corresponding authors

E-mail addresses: ladjarafi@gmail.com (A.Ladjarafi) and jean-francois.halet@univ-rennes1.fr (J.-F. Halet)

ABSTRACT

Quantum calculations were carried out on some pyrimidopyrimidine tautomeric heterocyclic derivatives both in gas phase and in solution in order to study the influence of the migration of hydrogen on their electronic and structural properties as well to highlight the effect of the solvent on the process of tautomerism. Results indicate that the electronic properties of the studied heterocycles are influenced by the nature of the solvent used. All tautomeric forms are more stable in H_2O and DMSO than in $CHCl_3$ and in the gas phase. The predominance of the *di-ketone* form in gas phase and solution is observed.

Keywords heterocycles, pyrimidopyrimidine, quantum calculations, solvent effect, tautomeric forms

1. Introduction

Because of their importance and their widespread presence in living organisms, substances based on pyrimidopyrimidines or tetra-azanaphthalenes − organic heterobicyclic compounds with a skeleton consisting of two pyrimidine rings that are ortho-fused to each other at any position − have aroused the interest of researchers in organic and pharmacology chemistry for several decades [1-12]. These molecules are well known for their important biological, biochemical and therapeutic properties as well as their rich and varied chemistry [10-23].

Several works reported on the preparation of pyrimidopyrimidines and their derivatives have demonstrated their antiallergic [11,18,24], anti-cancer [12,21,25-28], antihypertensive [15,29], anti-inflammatory utility and other antibiotic, antifungal and antibacterial properties [9-12,30-34]. Some pyrimidopyrimidines have fungicidal activities whereas others have been reported to be agricultural compounds [35-43]. Pyrimidopyrimidines also have veterinary uses as antibiotics, antiparasites, antipyretics, analgesics, analgesics and anti-inflammatories [44-46]. They also are found in meteorites, but scientists still do not know their origin [47].

In this work, we are interested in the theoretical study of the influence of proton transfer on the electronic and structural properties of one hypothetical pyrimidopyrimidine derivative, namely the pyrimido[5,4-*d*]pyrimidine-2,6(1*H*,3*H*,5*H*,7*H*)-dione $C_6N_4H_6O_2$ (PPD, Figure 1). The choice of this derivative was guided by the large number of experimental studies on the pharmacological and therapeutic properties of the related heterocyclic dihydropyrimidinone (DHPM) and its derivatives [48-58], arousing our interest in testing the possible fusion of two heterocycles and subsequently study its electronic properties. In this PPD species, the transfer of one proton can theoretically take place from the NH group to one of the neighboring oxygen atoms (having two lone electron pairs), thus leading to a mixture of several *keto* and *enol* forms called *tautomers*. Our interest then focused on the theoretical study in solution of different tautomeric pairs to prove the effect of the solvent on the tautomeric process encountered in this type of keto-enol tautomerization equilibrium. Three solvents of different polarity were chosen, those mostly used in synthesis which strongly differ by their dielectric constants, as chloroform ($CHCl_3$), a non-polar solvent of low dielectric constant ($\varepsilon = 4.8$), dimethylsulfoxide (C_2H_6OS, DMSO), a polar solvent of medium dielectric constant ($\varepsilon = 46.7$) and water (H_2O), a polar solvent of high dielectric constant ($\varepsilon = 80$) – the gas phase is taken as a reference with a dielectric constant ($\varepsilon = 1$). The different equilibria of the tautomers studied here are shown in Figure 1.

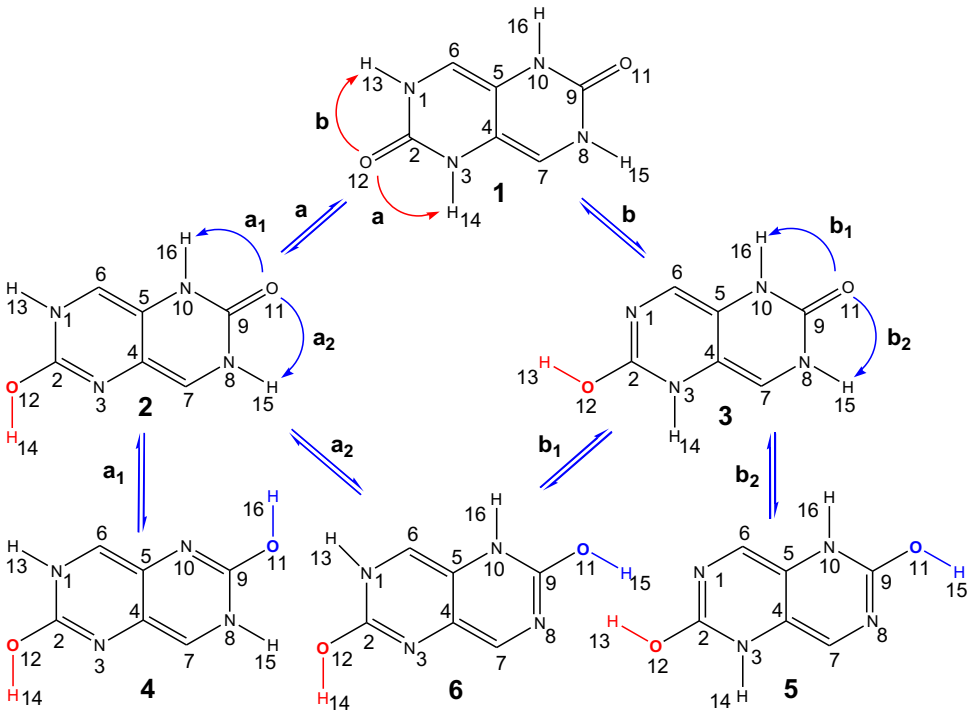

Fig. 1. Different tautomer equilibria studied in this article.

2. Computational Details

Calculations were carried out using three methods, namely the post-Hartree-Fock Moller-Plesset (MP2) method [59], and the density functional theory (DFT) method [60,61] using two functionals, the B3LYP (Becke's three-parameter exchange functional in conjunction with the Lee-Yang-Parr correlation functional [62] with Lee-Yang–Parr [63]) and the M06-2X [64] correlational functional. In all cases, a 6-311++G** basis set was used [65]. Calculations were performed first in the gas phase and then in the presence of three solvents ($CHCl_3$, DMSO, and H_2O) using the polarizable continuum model (PCM) [66,67]. Atomic charges were analyzed using two different approaches, namely the Natural Bond Orbital (NBO) analysis [68,69] and the atomic polar tensor (APT) analysis [70,71]. Full geometric optimizations were performed, followed by frequency calculations to ensure the nature of energy minima and transition states. All calculations were carried out with the *Gaussian*16 package [72]. Representation of molecular structures and molecular orbitals was performed using the *GaussView* [73] and *ChemDraw* programs [74].

3. Results and discussion

3.1. Stability of pyrimidopyrimidines

The pyrimidopyrimidine tautomeric molecules studied here exhibit the phenomenon of tautomerism, which appears when one of the hydrogen atoms can occupy different positions in a given skeleton (H_{13}, H_{14}, H_{15}, or H_{16} in Fig. 1). Migration of one of these hydrogen atoms create different structures in equilibrium, the composition of the tautomeric mixture of which is often difficult to determine experimentally [75]. Knowledge of the relative stabilities of tautomeric forms of these heterocyclic molecules as well as the conversion from one form to another are important from the point of view of structural chemistry. Moreover, the geometric and electronic structures as well as the thermodynamical stability of the tautomeric forms provide a basis for understanding their biological activities and lead to the determination of their pharmacological properties.

First, a conformational study was performed at the B3LYP/6-311++G** level on compounds **2**-**6** containing OH group(s) to find their most stable structures, varying the H-O-C-N dihedral angle (τ) from 0 to 180°. The most stable forms – we checked that they were genuine minima on the potential energy surface – and their relative free energies are shown in Fig. 2 (see also Fig. S1, Supporting Information). Two possible conformations were found for **2** and **3** ($\tau = 0°$ (**2a** and **3a**) and 180° (**2b** and **3b**)). For compounds **4**, **5**, and **6**, the variation of the dihedral angles H_{14}-O_{12}-C_2-N_3, H_{13}-O_{12}-C_2-N_1, H_{16}-O_{11}-C_9-N_{10} and H_{15}-O_{11}-C_9-N_8 from 0° to 180° leads to four possible conformers (two being identical in the case of **4** and **5**). It turns out that conformers *a* are substantially more stable than the other ones (see Fig. 2). Therefore, in the following compounds (**2a**, **3a**, **4a**, **5a** and **6a**) will subsequently be called **2**, **3**, **4**, **5**, and **6**, respectively.

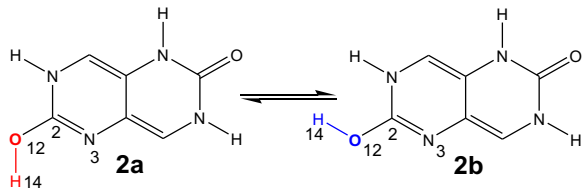

ΔG_{2a}=0.0 kcal.mol^{-1} ΔG_{2b}=7.1 kcal.mol^{-1}

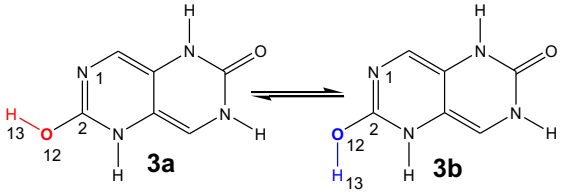

ΔG_{3a}=0.0 kcal.mol^{-1} ΔG_{3b}=8.5 kcal.mol^{-1}

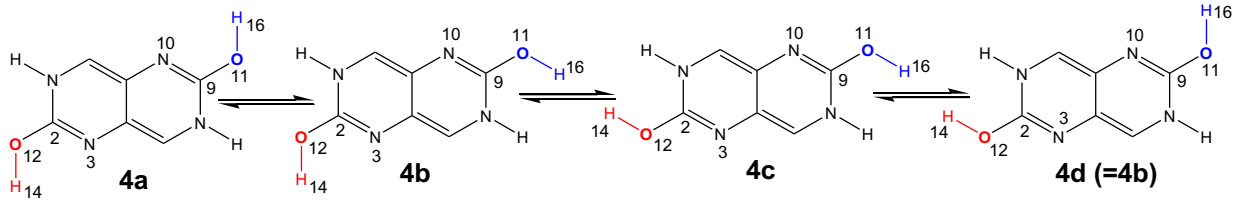

ΔG_{4a}=0.0 kcal.mol^{-1} ΔG_{4b}=7.2 kcal.mol^{-1} ΔG_{4c}=15.1 kcal.mol^{-1} ΔG_{4d}=7.2 kcal.mol^{-1}

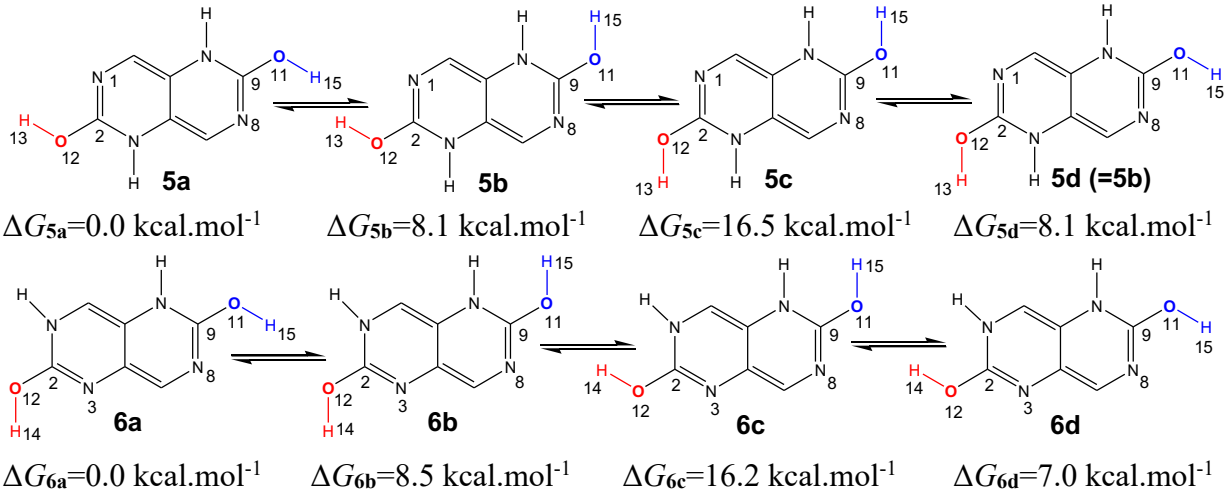

Fig. 2. Possible conformers of tautomeric forms **2-6** and their relative free energy computed in gas phase computed at the B3LYP/6-311++G** DFT level.

Full optimization calculations of geometries of the gas phase most stable conformers, hereafter denominated **2**, **3**, **4**, **5,** and **6**, were also carried out in the presence of three solvents ($CHCl_3$, DMSO and H_2O) at the MP2, B3LYP and M06-2X levels of theory for comparison (Fig. 3). The analysis of relative Gibbs free energies obtained in the gas phase and in solution by the three methods indicates the same order of stability (Table 1, see also Table S1, Supporting Information). The conformal compound *di-ketone* **1** is thermodynamically the most stable species in both gas phase and solution, followed by the tautomers *enols* **2** and **3** then followed by the *dienols* **4**, **5**, and **6**, respectively. The stability of the compounds obtained is then in the following decreasing order: **1** > **2** > **3** > **4** > **5** > **6**. Compound **6** is therefore the least stable. This result indicates that the migration of a hydrogen atom from the *imine* function to an oxygenated substituent decreases the stability of the compounds. This decrease becomes more significant in the case of *dienols* **4**, **5**, and **6** where there is a transfer of two protons.

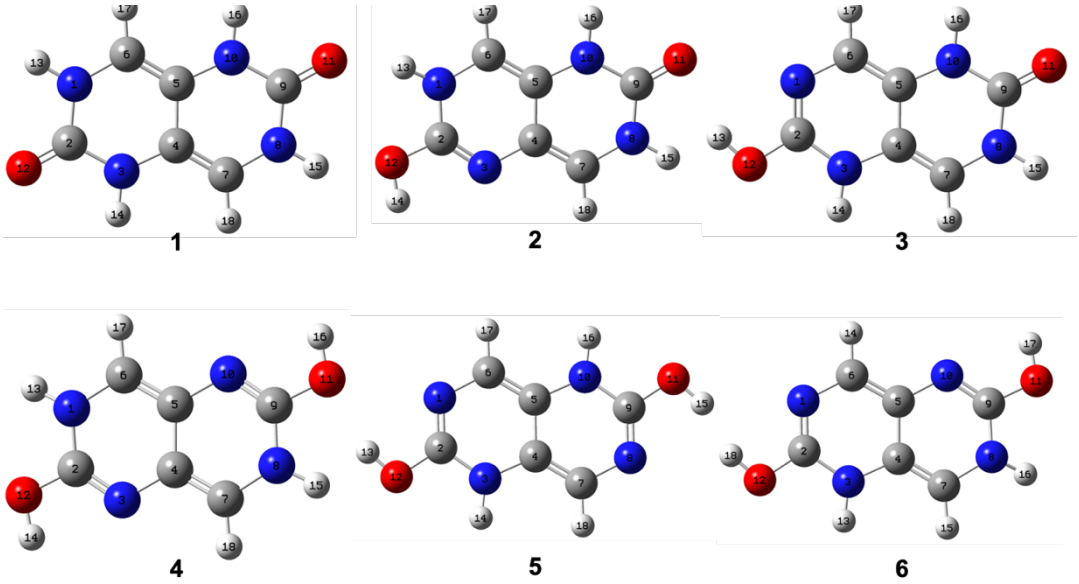

Fig. 3. Optimized structures of compounds **1-6** computed at the B3LYP/6-311++G** level in gas phase.

Table 1

Relative Gibbs free energies $\Delta\Delta G^{\ddagger}$ (in kcal.mol^{-1}) in gas phase and in solvent calculated using M06-2X, B3LYP (underlined) and MP2 (values in brackets) methods.

Cmpd	**1**	**2**	**3**	**4**	**5**	**6**
gas	0.0 0.0 (0.0)	10.5 [a] 12.7 [b] (10.7) [c]	11.5 13.7 (11.5)	22.2 26.1 (22.4)	24.0 28.1 (23.8)	24.4 28.4 (24.2)
$CHCl_3$	0.0 0.0 (0.0)	11.6 13.5 (10.8)	13.8 15.8 (12.9)	25.2 29.5 (24.2)	27.7 31.7 (26.0)	27.5 31.4 (25.8)
DMSO	0.0 0.0 (0.0)	12.4 14.4 (11.4)	14.5 16.5 (13.3)	26.3 30.3 (24.4)	29.3 33.2 (26.9)	28.2 32.1 (26.0)
H_2O	0.0 0.0 (0.0)	12.4 14.5 (11.5)	14.5 16.5 (13.3)	26.4 30.3 (24.4)	29.3 33.3 (27.0)	28.2 32.2 (26.0)

[a] $\Delta G_2^{\text{M06-2X}} - \Delta G_1^{\text{M06-2X}}$; [b] $\Delta G_2^{\text{B3LYP}} - \Delta G_1^{\text{B3LYP}}$; [c] $\Delta G_2^{\text{MP2}} - \Delta G_1^{\text{MP2}}$.

Table 2

Solvation free energies ($\Delta G_{sol}^{\ddagger}$, in kcal.mol^{-1}) calculated using M06-2X, B3LYP (underlined) and MP2 (in brackets) methods.

Cmpd	**1**	**2**	**3**	**4**	**5**	**6**
gas	0.0 0.0 (0.0)	0.0 0.0 (0.0)	0.0 0.0 (0.0)	0.0 0.0 (0.0)	0.0 0.0 (0.0)	0.0 0.0 (0.0)
$CHCl_3$	-10.0 [a]	-8.2	-8.2	-6.5	-6.5	-7.0

	-10.1 [b] (-8.2) [c]	-8.3 (-7.1)	-8.3 (-7.1)	-6.5 (-6.1)	-6.5 (-6.0)	-7.0 (-6.6)
DMSO	-14.0 -14.1 (-11.4)	-11.5 -11.5 (-9.9)	-11.5 -11.6 (-9.9)	-9.2 -9.1 (-8.5)	-9.1 -9.1 (-8.4)	-10.0 -10.0 (-9.2)
H_2O	-14.1 -14.3 (-11.6)	-11.7 -11.7 (-10.1)	-11.7 -11.7 (-10.1)	-9.3 -9.2 (-8.6)	-9.2 -9.2 (-8.5)	-10.2 -10.1 (-9.4)

[a] $\Delta G_{sol}^{\ddagger} = \Delta G_{CHCl_3}^{M06\text{-}2X} - \Delta G_{gas}^{M06-2X}$; [b] $\Delta G_{sol}^{\ddagger} = \Delta G_{CHCl_3}^{B3LYP} - \Delta G_{gas}^{B3LYP}$; [c] $\Delta G_{sol}^{\ddagger} = \Delta G_{CHCl_3}^{MP2} - \Delta G_{gas}^{MP2}$.

Results shown in Table 2, indicate that the solvation free energies of the studied species increase when passing from the gaseous state to the solution state and this for the three methods. Thus, the tautomers are more stable in water than in DMSO and then in $CHCl_3$, respectively. This increase is proportional, as expected, to the polarity of solvents used. By way of example using the M06-2X method, the presence of solvent provides compound **1** with a solvation free energy gain of 10.0, 14.0 and 14.1 kcal/mol in $CHCl_3$, DMSO and H_2O, respectively. The solvation free energy results obtained by the M06-2X and B3LYP methods are similar for each solvent. For example, for compound **5** the energy gain between the gas phase and the three solvents is respectively 6.5, 9.1 and 9.2 kcal/mol with M06-2X and B3LYP, respectively. The solvation free energy values obtained in the solvent H_2O are very close to those obtained in DMSO. The solvation free energies results obtained from the three methods are proportional to each other. For example, the proportionality coefficient calculated by dividing the values obtained in MP2 by those obtained in B3LYP is the same (99.728×10^{-2}) for all phases (see Table S1, Supporting Information). The comparison carried out between the Gibbs free energies obtained with the M06-2X and those obtained with B3LYP in gas phase and in solution gave a very good correlation between both methods with determination coefficients $R^2 \simeq 1$ (Fig. 4).

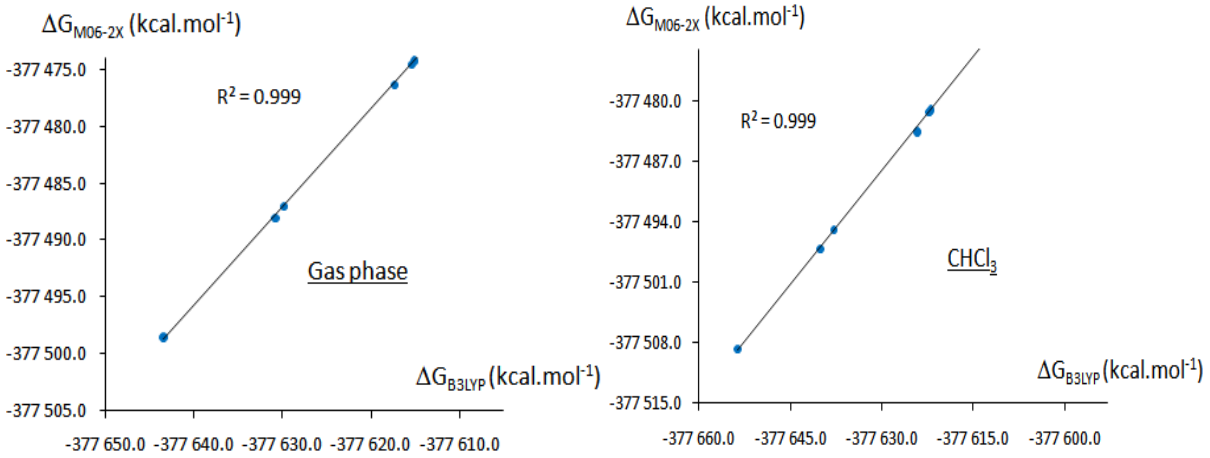

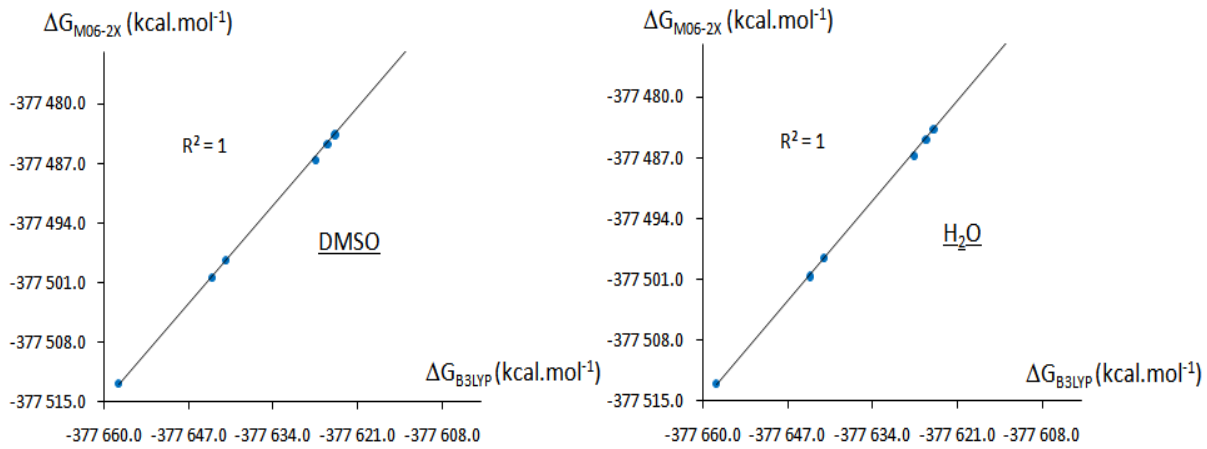

Fig. 4. Correlation diagram between B3LYP computed and M06-2X computed Gibbs free energies in gas phase and in solution.

3.2. Orbital analysis

The computed energies of the highest occupied molecular orbital (HOMO) and the lowest unoccupied molecular orbital (LUMO), as well as the HOMO-LUMO gap of compounds **1-6** obtained after complete optimization in the gas phase and in solution using the three methods M06-2X, B3LYP and MP2 are given in Table 3 and Fig. 5. Results indicate that the solvent hardly influences the HOMO-LUMO gaps. Comparable HOMO-LUMO gaps are computed in both phases and for the three methods for all compounds. The nodal properties of the HOMO and LUMO of **1-6** are shown in Fig. 5.

Both HOMOs and LUMOs are heavily distributed over the heterocycles. The Fig. 5 shows that the HOMO and LUMO of the tautomers **1-6** are mainly localized on the two pyrimidine rings, involving an important contribution of the nitrogen atoms, indicating that the two pyrimidine rings of the tautomers **1-6** are good π electrons donors.

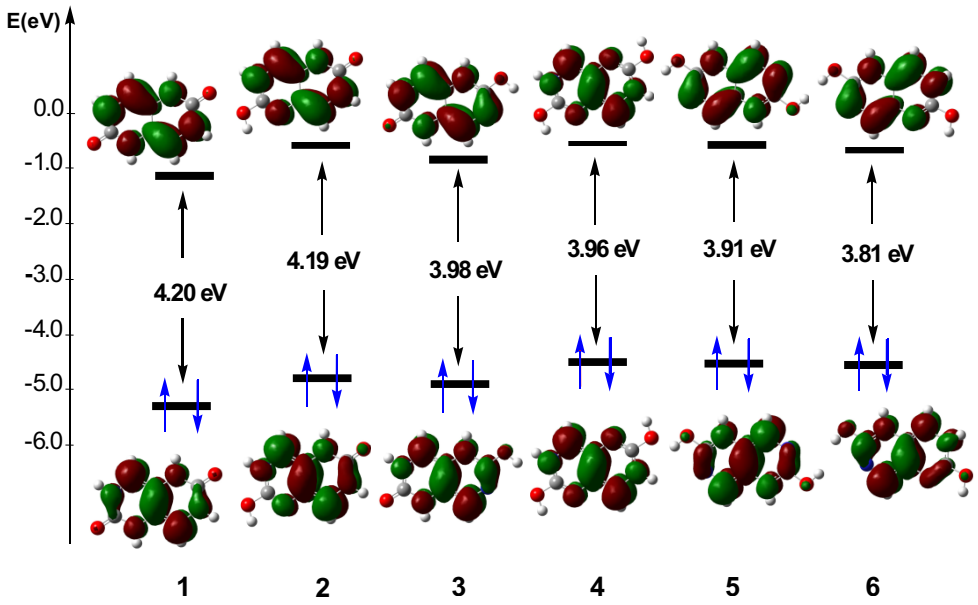

Fig. 5. Energies and nodal properties of the HOMO and LUMO of the tautomers **1**-**6** computed at the B3LYP/6-311++G** DFT level in the gas phase. Contour isodensity values: ± 0.05 $(e/bohr^3)^{1/2}$.

Compound **1** shows the highest HOMO-LUMO energy gap, reflecting its low chemical reactivity and high kinetic stability, indicating also that **1** is a hard compound and it is difficult to polarize because it needs more energy for excitation. On the other hand, compound **6** has the smallest HOMO-LUMO gap. It should therefore be the least stable (more reactive) compound. As a result, the chemical reactivity of the studied compounds increases as follows: **1** < **2** < **3** < **4** < **5** < **6**, and the kinetic stability decreases in the reverse order: **1** > **2** > **3** > **4** > **5** > **6**.

As expected, the HOMO-LUMO gaps obtained by MP2 are largely overestimated and practically twice those obtained with B3LYP and larger by 2.5 eV on average than those obtained with the M06-2X method. As expected, this is due to the positive energies of the MP2-computed LUMOs. Positive values for the LUMOs mean that the attachment of an electron to these molecules is energetically unfavorable. We also observe, with all methods, that compound **1** with the lowest LUMO energy has a strong electronic affinity in the gas phase and in solution, revealing its important electro-acceptor character.

Table 3

M06-2X-, B3LYP- and MP2-computed energies of the HOMO and LUMO (in eV), HOMO-LUMO gaps (in eV) in gas phase and in the solvents $CHCl_3$ (underlined), DMSO (in italics) and H_2O (in brackets).

Cmpd	**1**	**2**	**3**	**4**	**5**	**6**
M06-2X						
E_{HOMO}/E_{LUMO}	-6.50/-0.38 <u>-6.37/-0.14</u> *-6.33/-0.07* (-6.33)/(-0.07)	-6.10/-0.33 <u>-6.05/-0.13</u> *-6.05/-0.07* (-6.05)/(-0.07)	-6.03/-0.30 <u>-5.99/-0.11</u> *-6.01/-0.06* (-6.01)/(-0.06)	-5.72/-0.16 <u>-5.76/-0.08</u> *-5.79/-0.07* (-5.79)/(-0.07)	-5.60/-0.12 <u>-5.67/-0.06</u> *-5.73/-0.05* (-5.73)/(-0.05)	-5.71/-0.30 <u>-5.72/-0.10</u> *-5.74/-0.07* (-5.74)/(-0.07)
$\Delta E_{HOMO-LUMO}$	6.11 <u>6.23</u> *6.26* (6.26)	5.77 <u>5.92</u> *5.98* (5.98)	5.73 <u>5.89</u> *5.95* (5.95)	5.56 <u>5.67</u> *5.72* (5.72)	5.48 <u>5.63</u> *5.69* (5.69)	5.41 <u>5.62</u> *5.67* (5.67)
B3LYP						
E_{HOMO}/E_{LUMO}	-5.25/-1.05 <u>-5.10/-0.88</u> *-5.06/-0.82* (-5.06)/(-0.82)	-4.81/-0.62 <u>-4.76/-0.57</u> *-4.77/-0.57* (-4.77)/(-0.58)	-4.88/-0.90 <u>-4.82/-0.84</u> *-4.81/-0.82* (-4.81)/(-0.82)	-4.49/-0.53 <u>-4.47/-0.51</u> *-4.51/-0.57* (-4.52)/(-0.57)	-4.50/-0.59 <u>-4.53/-0.64</u> *-4.55/-0.68* (-4.55)/(-0.68)	-4.52/-0.71 <u>-4.55/-0.72</u> *-4.58/-0.74* (-4.58)/(-0.74)
$\Delta E_{HOMO-LUMO}$	4.20 <u>4.22</u> *4.24* (4.24)	4.19 <u>4.19</u> *4.20* (4.19)	3.98 <u>3.98</u> *3.99* (3.99)	3.96 <u>3.95</u> *3.94* (3.94)	3.91 <u>3.89</u> *3.87* (3.87)	3.81 <u>3.83</u> *3.84* (3.84)
MP2						
E_{HOMO}/E_{LUMO}	-7.50/1.09 <u>-7.29/1.30</u> *-7.23/1.37* (-7.23)/(1.37)	-6.97/1.58 <u>-6.93/1.62</u> *-6.94/1.61* (-6.94)/(1.61)	-6.47/2.05 <u>-6.58/1.92</u> *-6.64/1.86* (-6.64)/(1.85)	-6.94/1.30 <u>-6.87/1.39</u> *-6.86/1.40* (-6.86)/(1.40)	-6.48/1.67 <u>-6.54/1.60</u> *-6.58/1.55* (-6.58)/(1.55)	-6.38/1.58 <u>-6.44/1.52</u> *-6.48/1.49* (-6.48)/(1.49)
$\Delta E_{HOMO-LUMO}$	8.59 <u>8.59</u> *8.60* (8.60)	8.55 <u>8.55</u> *8.55* (8.55)	8.52 <u>8.50</u> *8.50* (8.49)	8.24 <u>8.26</u> *8.26* (8.26)	8.15 <u>8.14</u> *8.13* (8.13)	7.96 <u>7.96</u> *7.97* (7.97)

3.3. Free energy profiles

For the research of the transition states connecting two tautomers, we used the B3LYP method (Table 4), which is considerably less costly in computation time compared to M06-2X especially to MP2 and which is known to qualitatively reproduce the free energy profiles of reactions in organic chemistry and find in particular the main intermediate and transition states. The results given in Table 4 show that the presence of the solvent has a little influence on the free energy barriers which increase slightly by approximately 2 kcal/mol on going from the gas phase to solution. The values of the free energy barriers in water (H_2O) are close to those obtained in DMSO. Vibration frequency calculations of the transition states obtained

(Fig. 6) show that each of these states has a significant imaginary frequency (see Table S2 and Fig. S2, Supporting Information), which means that they really represent energy maxima.

Table 4

Gibbs free energies ($G_{TS}^{\ddagger}$ in kcal.mol^{-1}) and free energy barriers ($\Delta G_{a\leftrightarrow b}$, in kcal.mol^{-1}) of the transition states in gas phase and in solution, obtained by the B3LYP method.

	gas		$CHCl_3$		DMSO		H_2O	
	$G_{TS_{a\leftrightarrow b}}^{gas}$	$\Delta G_{a\leftrightarrow b}^{gas}$	$G_{TS_{a\leftrightarrow b}}^{CHCl_3}$	$\Delta G_{a\leftrightarrow b}^{CHCl_3}$	$G_{a\leftrightarrow b}^{DMSO}$	$\Delta G_{a\leftrightarrow b}^{DMSO}$	$G_{a\leftrightarrow b}^{H_2O}$	$\Delta G_{a\leftrightarrow b}^{H_2O}$
$TS_{1\leftrightarrow 2}$	-377 597.40	46.0	-377 376.79	47.8	-377 609.02	48.7	-377 609.18	48.3
$TS_{1\leftrightarrow 3}$	-377 595.25	48.2	-377 376.62	49.9	-377 606.85	50.8	-377 607.04	50.7
$TS_{2\leftrightarrow 4}$	-377 584.93	45.8	-377 375.36	48.6	-377 593.85	49.4	-377 593.99	48.4
$TS_{2\leftrightarrow 6}$	-377 581.53	49.2	-377 375.34	51.7	-377 591.10	52.2	-377 591.24	51.3
$TS_{3\leftrightarrow 5}$	-377 582.80	38.0	-377 375.79	41.9	-377 592.58	44.2	-377 592.71	44.3
$TS_{3\leftrightarrow 6}$	-377 581.21	39.6	-377 375.69	44.0	-377 590.20	46.6	-377 590.34	46.7

$\Delta G_{a\leftrightarrow b}^{state} = G_{TS_{a\leftrightarrow b}}^{state} - G_{a}^{state}$ (state = gas, $CHCl_3$, DMSO, H_2O).

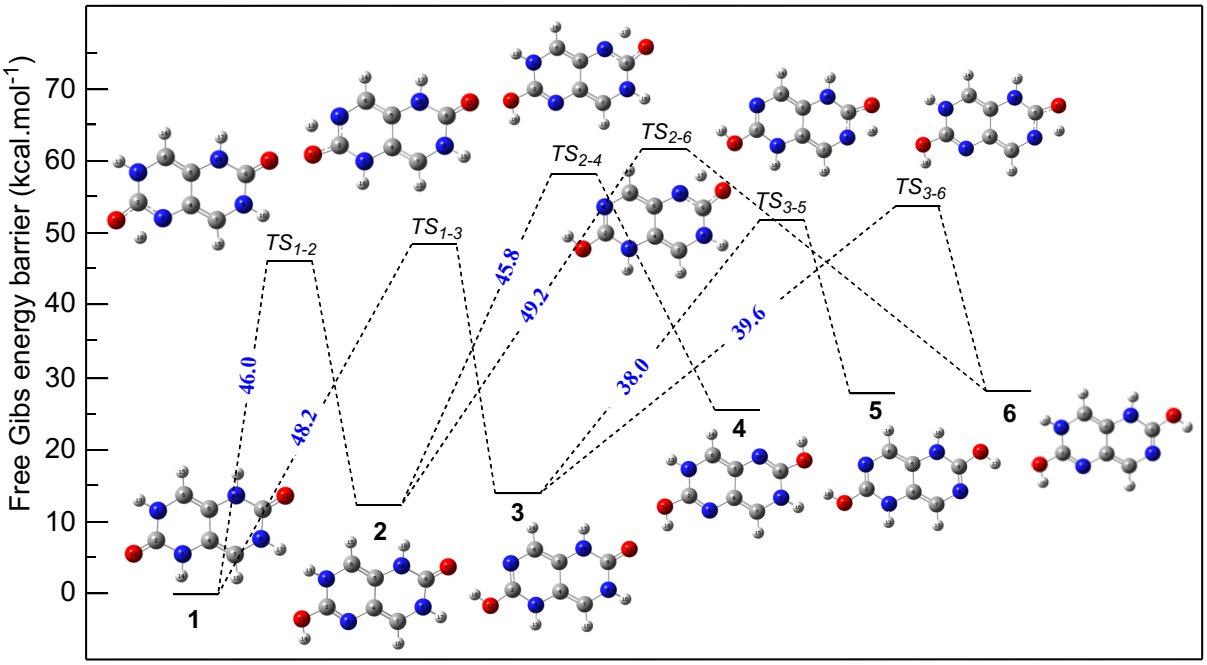

Fig. 6. Energy profile of the tautomers **1-6** studied in the gas phase.

3.4. Thermodynamic quantities of tautomeric couples

Thermodynamic quantities obtained of tautomeric couples were calculated at $T = 298.15$ K and under 1 atm pressure (Table 5) for compounds **1**-**6**. In order to determine the influence of the solvent on the reactivity, the effect of the solvent was taken into account using the PCM model [67,68] which has been widely used for the study of a large variety of molecules in solution and in the prediction of solvent effects [76-79]. Let us remind that the PCM model does not consider the presence of explicit solvent molecules; therefore, specific solute-solvent interactions are not defined and the studied solvation effects arise only from mutual solute-solvent electrostatic polarization.

Equilibrium constants were calculated as the difference between the Gibbs free energies (or free enthalpies) $\Delta G°_{ab}$ of the two tautomers *a* and *b* (*a*, *b* = **1**-**6**) by the relation:

$$\Delta G°_{ab} = \Delta H°_{ab} - T\Delta S°_{ab} \qquad (1)$$

where $\Delta H°_{ab}$ et $\Delta S°_{ab}$ represent the difference of the standard enthalpy and the standard entropy of the two forms *a* and *b*, respectively.

The equilibrium constant was calculated with the relation:

$$K_{ab} = \exp(-\Delta G°_{ab}/RT) \qquad (2)$$

where *R* is the ideal gas constant and *T* is the absolute temperature.

Table 5

Variation of enthalpy ($\Delta H°$, in kcal/mol), entropy ($\Delta S°$, in cal/mol.K), Gibbs free energy ($\Delta G°_{ab}$, in kcal/mol) and equilibrium constant (K_{ab}) in gas phase and in solution, calculated via B3LYP and MP2 (in brackets) methods.

	$\Delta H°$	$\Delta S°$	$\Delta G°_{ab}$	K_{ab}	$\Delta H°$	$\Delta S°$	$\Delta G°_{ab}$	K_{ab}
	Gas				$CHCl_3$			
1↔2	11.99	-1.45	12.68	$5.08\ 10^{-10}$	13.72	1.73	13.60	$1.07\ 10^{-10}$
	(10.17)	(-4.00)	(11.48)	($3.86\ 10^{-9}$)	(10.85)	(1.20)	(11.03)	($8.16\ 10^{-9}$)
1↔3	13.59	-0.98	14.12	$4.47\ 10^{-11}$	15.36	-0.88	15.88	$2.27\ 10^{-12}$
	(11.43)	(-2.95)	(12.53)	($6.56\ 10^{-10}$)	(13.14)	(2.98)	(11.89)	($1.93\ 10^{-9}$)
2↔4	13.12	-0.51	13.55	$1.16\ 10^{-10}$	14.79	-1.11	15.53	$4.14\ 10^{-12}$
	(11.46)	(-2.74)	(12.39)	($8.23\ 10^{-10}$)	(12.41)	(-2.04)	(13.25)	($1.95\ 10^{-10}$)
2↔6	15.70	-1.53	16.39	$9.64\ 10^{-13}$	16.88	-2.91	18.03	$6.10\ 10^{-14}$
	(13.49)	(-1.73)	(14.21)	($3.81\ 10^{-11}$)	(14.02)	(-1.16)	(14.62)	($1.92\ 10^{-11}$)
3↔5	13.87	-1.68	14.60	$1.97\ 10^{-11}$	15.62	-1.09	16.25	$1.22\ 10^{-12}$
	(11.64)	(-0.33)	(12.04)	($1.48\ 10^{-9}$)	(12.73)	(-0.98)	(13.32)	($1.71\ 10^{-10}$)
3↔6	14.11	-2.00	14.95	$1.10\ 10^{-11}$	15.24	-0.31	15.74	$2.89\ 10^{-12}$
	(12.23)	(-2.77)	(13.16)	($2.24\ 10^{-10}$)	(12.74)	(-2.93)	(13.76)	($8.12\ 10^{-11}$)

	DMSO				H_2O			
1↔2	14.37 (12.27)	1.46 (0.57)	14.37 (11.59)	$2.92\ 10^{-11}$ ($3.19\ 10^{-9}$)	14.41 (12.29)	1.40 (0.54)	14.41 (11.62)	$2.73\ 10^{-11}$ ($3.01\ 10^{-9}$)
1↔3	16.01 (13.55)	-0.89 (2.57)	16.57 (12.38)	$7.12\ 10^{-13}$ ($8.42\ 10^{-10}$)	16.04 (13.57)	-0.89 (2.54)	16.59 (12.41)	$6.84\ 10^{-13}$ ($7.99\ 10^{-10}$)
2↔4	15.45 (12.74)	0.43 (-1.80)	15.74 (13.54)	$2.91\ 10^{-12}$ ($1.18\ 10^{-10}$)	15.47 (12.75)	0.60 (-1.79)	15.71 (13.54)	$3.05\ 10^{-12}$ ($1.19\ 10^{-10}$)
2↔6	17.20 (14.11)	-1.43 (-0.93)	17.91 (14.67)	$7.48\ 10^{-14}$ ($1.77\ 10^{-11}$)	17.20 (14.11)	-1.24 (-0.91)	17.87 (14.66)	$7.88\ 10^{-14}$ ($1.78\ 10^{-11}$)
3↔5	16.34 (13.17)	-1.02 (-1.22)	16.91 (13.83)	$4.02\ 10^{-13}$ ($7.25\ 10^{-11}$)	16.37 (13.19)	-1.02 (-1.23)	16.95 (13.86)	$3.72\ 10^{-13}$ ($6.95\ 10^{-11}$)
3↔6	15.56 (12.83)	0.92 (-2.92)	15.71 (13.88)	$3.06\ 10^{-12}$ ($6.70\ 10^{-11}$)	15.57 (12.84)	1.05 (-2.92)	15.69 (13.88)	$3.15\ 10^{-12}$ ($6.72\ 10^{-11}$)

Results in the gas phase and in all solvents correctly confirm the predominance of **1** against **2**, **2** against **4** and **6**, and **3** against **5** and **6**. They also indicate that the solvents H_2O and DMSO and to a lesser extent $CHCl_3$ increase the variation of the enthalpy and the Gibbs free energy compared to the gas phase. The values of the variation of entropy in the gas phase are all negative, indicating that the disorder of these systems decreased going from one tautomer to another.

3.5. Dipole moments

Dipole moments obtained for compound **2**, **3**, **4** and **6** via the M06-2X, B3LYP and MP2 methods increase from the gas phase to solution (Table 6). This change is mainly due to the modification of the electronic distribution. They are sensitive to solvent polarity, being, as expected, higher in water (H_2O) than in DMSO and in the less polar solvent $CHCl_3$. Compound **3** is the most polar species, leading to a clear dissymmetry in the atomic charge distribution, resulting in a high polarity of the N−H and O−H bonds. While compound **4** is the least polar, note that, as expected, symmetric compounds **1** and **5** are non-polar, so they have a better distribution of partial atomic charges.

Table 6
Dipolar moments (in Debye) in the gas phase and solution, calculated via M06-2X, B3LYP (underlined) and MP2 (in brackets) methods.

Cmpd	**1**	**2**	**3**	**4**	**5**	**6**
gas	0.00 <u>0.00</u> (0.00)	3.63 <u>3.66</u> (3.71)	3.96 <u>3.96</u> (4.30)	0.41 <u>0.38</u> (0.46)	0.00 <u>0.00</u> (0.00)	3.20 <u>3.25</u> (3.22)

$CHCl_3$	0.00 0.00 (0.00)	4.91 4.93 (4.75)	4.99 5.01 (5.17)	0.66 0.67 (0.68)	0.00 0.00 (0.00)	4.54 4.62 (4.39)
DMSO	0.00 0.00 (0.00)	5.42 5.46 (5.19)	5.41 5.44 (5.51)	0.97 0.98 (0.90)	0.00 0.00 (0.00)	5.24 5.33 (4.98)
H_2O	0.00 0.00 (0.00)	5.45 5.48 (5.21)	5.43 5.46 (5.52)	1.17 1.16 (1.21)	0.00 0.00 (0.00)	5.28 5.37 (5.02)

3.6. Intramolecular distances and bond indices

Pertinent interatomic distances calculated via the B3LYP method (Table 7) show that the distance C_2–O_{12} lengthens from 1.218 Å in compound **1** (double bond character) to 1.350 Å (simple bond character) in compounds **2**-**6**. The same thing is observed for the distance C_9–O_{11} which varied from a double bond (~ 1.218 Å) in compounds **1**-**3** to a simple bond (~ 1.350 Å) in compounds **4**-**6**. While the distances C_2–N_1, C_2–N_3, C_9–N_8 and C_9–N_{10} shorten from a single bond to a double bond upon migration of the protons (H_{13}, H_{14} or H_{15}, H_{16}) to one of the oxygen atoms O_{12} or O_{11}, respectively. Wiberg bond indices (WBI) [80] computed for the studied compounds (Table 7) confirm these interatomic distance variations. Each pair of bond atoms C_2–O_{12} (for **1**), C_9–O_{11} (for **1**-**3**), C_2–N_1 (for **1** and **5**), C_2–N_3 (for **2**, **4** and **6**), C_9–N_8 (for **5** and **6**) and C_9–N_{10} (for **4**), sharing a half-bond π, plus a σ bond giving these bonds a bonding index of approximately 1.6.

Table 7

Interatomic distances (Å) and Wiberg bond indices (in parenthesis) obtained via the B3LYP method.

Cmpd	**1**	**2**	**3**	**4**	**5**	**6**
N_1–H_{13}	1.007 (0.806)	1.007 (0.804)	2.400 (0.008)	1.007 (0.805)	2.304 (0.008)	1.008 (0.808)
N_3–H_{14}	1.009 (0.805)	2.288 (0.008)	0.992 (0.802)	2.279 (0.009)	1.009 (0.806)	2.280 (0.006)
N_8–H_{15}	1.007 (0.806)	1.007 (0.807)	0.994 (0.808)	1.007 (0.806)	2.304 (0.008)	2.304 (0.009)
N_{10}–H_{16}	1.009 (0.805)	1.009 (0.806)	0.994 (0.804)	2.279 (0.008)	1.009 (0.802)	1.009 (0.806)
C_2–O_{12}	1.218 (1.633)	1.350 (1.033)	1.353 (1.033)	1.350 (1.034)	1.351 (1.030)	1.350 (1.029)
C_9–O_{11}	1.218 (1.633)	1.219 (1.630)	1.218 (1.634)	1.350 (1.034)	1.351 (1.030)	1.351 (1.034)

C_2–N_1	1.376 (1.100)	1.363 (1.134)	1.279 (1.609)	1.358 (1.149)	1.277 (1.626)	1.365 (1.103)
C_2–N_3	1.386 (1.084)	1.281 (1.600)	1.398 (1.120)	1.284 (1.595)	1.371 (1.110)	1.281 (1.628)
C_9–N_8	1.376 (1.100)	1.373 (1.113)	1.406 (1.106)	1.358 (1.149)	1.277 (1.626)	1.277 (1.597)
C_9–N_{10}	1.386 (1.084)	1.389 (1.073)	1.404 (1.079)	1.284 (1.597)	1.371 (1.110)	1.372 (1.140)
O_{12}–H_{13}	2.483 (0.004)	2.403 (0.002)	0.973 (0.737)	2.404 (0.003)	0.967 (0.739)	2.397 (0.002)
O_{12}–H_{14}	2.450 (0.004)	0.967 (0.738)	2.444 (0.003)	0.967 (0.739)	2.388 (0.003)	0.967 (0.738)
O_{11}–H_{15}	2.483 (0.004)	2.484 (0.004)	2.516 (0.004)	2.404 (0.003)	0.967 (0.739)	0.967 (0.738)
O_{11}–H_{16}	2.450 (0.004)	2.445 (0.004)	2.506 (0.004)	0.967 (0.739)	2.388 (0.003)	2.384 (0.003)

3.7. Analysis of atomic charges

A study of the atomic charges in compounds **1-6** was carried out using two different approaches (NBO and APT (Atomic Polar Tensor)). In order to facilitate the comparison with the different tautomers studied, only the most representative values are gathered in Tables S3-S6 (Supporting Information). The atom numbering is as shown in Fig. 1. The results obtained with M06-2X, B3LYP and MP2 methods indicate that intra- and extra-cyclic heteroatoms (N_1, N_3, N_8, N_{10}, O_{11} and O_{12}) of all the compounds bear significant negative charges, due to their high electronegativity and therefore their high potential reactivity. The atomic charge of these and MP2) going from the gas phase to the solvents $CHCl_3$, DMSO and finally H_2O. This increase in atomic charges is proportional to the solvent polarity [81,82]. On the other hand, the atomic charges computed with the NBO approach show little dependence on the effect of the solvents between 0.002 and 0.006 Å. Nevertheless, the NBO and APT approaches show that the atoms C_2 and C_9 are the most positively charged, indicating therefore they are the sites for nucleophilic attack. On the contrary, the atoms O_{11} and O_{12} are the most negatively charged thus representing electrophilic attack sites.

4. Conclusion

This theoretical study on the electronic and structural properties of some tautomeric pyrimidopyrimidine derivatives in gas phase and in solution in order to study the influence of the migration of hydrogen atoms allowed us to determine the most stable structures and to study possible equilibrium displacements. The results obtained with the M06-2X, B3LYP, and

MP2 methods showed that the *keto* forms are more stable than the *enol* ones. Additionally, the large HOMO-LUMO gap computed for compound **1** shows its high kinetic stability and, consequently must the least reactive compound of the series. The influence of the solvents on the geometry, the stability and the reactivity, was discussed. Wiberg bond indices computed for the studied compounds confirm the interatomic distances variations of each pair of bond atoms. The atomic charges computed with the APT approach reflect their dependence on the effect of the solvents unlike the NBO analysis.

Declaration of competing interest

The authors declare that they have no known competing financial interests or personal relationships that could have appeared to influence the work reported in this paper.

Supplementary materials

Supplementary material associated with this article can be found, in the online version, at doi:xxx.

Références

[1] E.C. Taylor, R.J. Knopf, R.F. Meyer, A. Holmes, M.L. Hoefle, J. Am. Chem. Soc. 82 (1960) 5711–5718.

[2] R. Lichtner, W. Haarmann, Prog. Clin. Biol. Res. 89 (1982) 131–41.

[3] H. Gastpar, Laryngol. Rhinol. Otol. (Stuttg). 62 (1983) 578–85.

[4] R.B. Lichtner, G. Hutchinson, N. Wedderburn, K. Hellmann, Cancer Treat. Rev. 12 (1985) 221–234.

[5] R.B. Lichtner, G. Hutchinson, K. Hellmann, Eur. J. Cancer Clin. Oncol. 25 (1989) 945–951.

[6] I. Bellido, J.P. De La Cruz, F. Sánchez De La Cuesta, Methods. Find. Exp. Clin. Pharmacol. 13 (1991) 371–375.

[7] J.P. De La Cruz, A. Moreno, F. Mérida, J. García-Campos, F. Sánchez de la Cuesta, Pharmacol. Toxicol. 75 (1994) 250–254.

[8] J.P. De La Cruz, G. Ortega, F. Sánchez de la Cuesta, Biochem. Pharmacol. 47 (1994) 209–215.

[9] K. Seio, T. Kanamori, A. Ohkubo, M. Sekine, Synthesis and fluorescence properties of nucleosides with pyrimidopyrimidine-type base moieties, fluorescent analogs of biomolecular

building blocks, design and applications, First edition, Edited by Marcus Wilhelmsson and Yitzhak Tor., John Wiley & Sons, Inc, 2016, pp. 47-67.

[10] M. Monier, D. Abdel-Latif, A. El-Mekabaty and K.M. Elattar, RSC Adv. 9 (2019) 30835–30867.

[11] K. M. Elattar, B. D. Mert, M. Monier and A. El-Mekabaty, RSC Adv. 10 (2020) 15461–15492.

[12] J. Santos Cruz, A. Palermo de Aguiar, Mini-Rev. Med. Chem. (2021) 2138–2168.

[13] Y.S. Sanghvi, S.B. Larson, S.S. Matsumoto, L.D. Nord, D.F. Smee et al, J. Med. Chem. 32 (1989) 629–637.

[14] J.P. De La Cruz, T. Carrasco, G. Ortega, F. Sánchez de la Cuesta 27 (1992) 192–194.

[15] V.J. Ram, A. Goel, S. Sarkhel, P.R. Maulik, Bioorg. Med. Chem. 10 (2002) 1275–1280.

[16] M. Gohain, D. Prajapati, B.J. Gogoi, Jr S. Sandhu, Advanced online publication (Synlett) 7 (2004) 1179–1182.03.06.204

[17] T.A. Naik and K.H. Chikhalia, E-Journal of Chemistry 4 (2007) 60–66.

[18] H. Parveen, F. Hayat, A. Salahuddin, and A. Azam, Eur. J. Med. Chem. 45 (2010) 3497–3503.

[19] V. Sharma, N. Chitranshi, and A.K. Agarwal, Int. J. Med. Chem. (2014) 1- 31.

[20] R. Merugu, S. Garimella, D. Balla, K. Sambaru, Int. J. Pharmtech. Res. 6 (2015) 88–93.

[21] Y. Hao, J. Lyu, R. Qu, D. Sun, Z. Zhao, Z. Chen, J. Ding, H. Xie, Y. Xu & H. Li, Scientific. Repo. Rts. 7 (2017) 3830.

[22] W. Ettahiri, M. El Hafi, S. Lahmidi, N. Abad, Y. Ramli, L. El Ghayati & E. Essassi, J. Mar. Chim. Heterocycl. 19 (2020) 1–36.

[23] N. Kitamura, A.K. Ohnishi, Pyrimidopyrimidine derivatives, method for the production thereof, the pharmaceutical preparations containing them and their use as an anti-allergic agent, AT-51231-T, Nippon Zoki Pharmaceutical Co (JP), 1984.
https://patents.google.com/patent/EP0163599B1/en

[24] K. Smith, Pyrimidopyrimidine derivatives, EP 0 351 058 B1, European Patent Office, 1993. https://data.epo.org/gpi/EP0351058A1

[25] W. Coates, Chem. Abstr. 113 (1990) 40711.

[26] F.F. Solca, A. Baum, E. Langkopf, G. Dahmann, K.-H. Heider, F. Himmelsbach, and J.C.A. van Meel, J. Pharmacol. Exp. Ther. (JPET) 311 (2004) 502–509.

[27] T. Xu, L. Zhang, S. Xu, C.-Y. Yang, J. Luo, F.Ding, X. Lu, Y. Liu, Z. Tu, S. Li, D. Pei, Q. Cai, H. Li, X. Ren, S. Wang, K. Ding, Angew. Chem. Int. Ed. 52 (2013) 8387–8390.

[28] S.A. El-Kalyoubi, Chem. Cent. J. 12 (2018) 64.

[29] P. Raddatz, R. Bergmann, Chem. Abstr. 109 (1988) 54786.
[30] A.M. Thompson, D.K. Murray, W.L. Elliott, D.W. Fry, J.A. Nelson, H.D.H. Showalter, B.J. Roberts, P.W. Vincent, W.A. Denny, J. Med. Chem. 40 (1997) 3915–3925.
[31] D.W. Fry, J.A. Nelson, V. Slintak, P.R. Keller, G.W. Rewcastle, W.A. Denny, H.R. Zhou, A.J. Bridges, Biochem. Pharmacol. 54 (1997) 877–887.
[32] P. Sharma, N. Rane, V.K. Gurram, Bioorganic Med. Chem. Lett. 14 (2004) 4185–4190.
[33] M.A. Hala, M.S. Nashwa, A.E. Heba, Eur. J. Med. Chem. 46 (2011) 4566–4572.
[34] K.M. Elattar and B.D. Mert, RSC Adv., 6 (2016) 71827–71851.
[35] R.E. Hackler, G.P. Jourdan, fungicidaluse of pyridopyrimidine, pteridine, pyrimidopyrimidine, pyrimidopyridazine, and pyrimido-1,2,4-triazine derivatives, U.S. Patent, N° 5,034,393, Dowelanco, Indianapolis, Ind., 1991.
https://patents.justia.com/patent/5034393
[36] R. Hirsh., T. Terenes, K. Haberer, K.L. Kratz, Sci. Total Environ. 225 (1999) 109–118.
[37] E.J.E. Freyne, M. Willems, P.H. Stork, V.S. Poncelet et all, Pyrido and pyrimidopyrimidine derivatives as anti-proliferative agents, Brevet Canadian N° 2549869C, Office de la propriété intellectuelle du Canada, 2005.
https://patents.google.com/patent/CA2549869A1
[38] K. Mazaahir, S. Kavita, and K.Z. Shuchi, Naturforsch. 62 (2007) 732–736.
[39] M. Wenyan, L. Guihong, W. Tao, H. Hongwu, J. Fluor. Chem. 129 (2008) 519–523.
[40] S.L. Kuchta, A.J. Cessna, J.A. Elliot, K.M. Peru, and J.V. Headley, J. Environ. Qual. 38 (2009) 1719–1727.
[41] T. Wang, X. Liu, J. Luo, X. Xu, D. Yu, Chinese J. Org. Chem., 31 (2011) 1773–1784.
[42] S. Yun-Lian, H. Tao, N. Xu-Liang, P. Da-Yong, L. Jin-Chuan and L. Bao-Tong, Z. Kristallogr. NCS 234 (2019) 331–332.
[43] N.A.A. Elkanzi, Orient. J. Chem. 36 (2020) 1001–1015.
[44] M.A. Hala and M.S. Nashwa, Int. J. Adv. 2 (2014) 694–702.
[45] J.P. De La Cruz, A. Moreno, F. Mérida, J. García Campos, F. Sánchez de la Cuesta, Thromb. Res. 81 (1996) 327–37.
[46] H.-J. Yang, L. Bogomolnaya, M. McClelland, H. Andrews-Polymenis, PLoS One, 12 (2017) 1-15, e0183751.
[47] M.P. Callahan, K.E. Smith, H.J. Cleaves, J. Ruzicka, J.C. Stern, D.P. Glavin, C.H. House, J.P. Dworkin, Proc. Natl. Acad. Sci. USA, 108 (2011) 13995–13998.
[48] A. De Fatima, T.C. Braga, L.D.S. Neto, B.S. Terra, B.G. Oliveira, D.L. da Silva, L.V. Modolo, J. Adv. Res. 6 (2015) 363–373.

[49] H. Nagarajaiah, A. Mukhopadhyay, J.N. Moorthy, Tetrahedron Lett. 57 (2016) 5135–5149.

[50] N. Pagano, P. Teriete, M.E. Mattmann, L. Yang, B.A. Snyder, Z. Cai, M.L. Heli, N.D.P. Cosford, Bioorg. Med. Chem. 25 (2017) 6248–6265.

[51] X. Zhu, G. Zhao, X. Zhou, X. Xu, G. Xia, Z. Zheng, L. Wang, X. Yang, L. Song, Bioorg. Med. Chem. Lett. 20 (2010) 299–301.

[52] M. Matias, G. Campos, A.O. Santos, A. Falcão, S. Silvestre, G. Alves, RSC. Adv. 6 (2016) 84943–84958.

[53] G. Lauro, M. Strocchia, S. Terracciano, I. Bruno, K. Fischer, C. Pergola, O. Werz, R. Riccio, G. Bifulco, Eur. J. Med. Chem. 80 (2014) 407–415.

[54] K.L. Dhumaskar, S.N. Meena, S.C. Ghadi, S.G. Tilve, Bioorg. Med. Chem. Lett. 24 (2014) 2897–2899.

[55] T.N. Akhaja, J.P. Raval, Eur. J. Med. Chem. 46 (2011) 5573–5579.

[56] M.Y. Wani, A. Ahmad, S. Kumar, A.J.F.N. Sobral, Microb. Pathog. 105 (2017) 57–62.

[57] R.W. Lewis, J. Mabry, J.G. Polisar, K.P. Eagen, B. Ganem, G.P. Hess, Biochemistry 49 (2010) 4841–4851.

[58] J.D. Bhatt, C.J. Chudasama, K.D. Patel, Arch. Pharm. 350 (2017) 1700088.

[59] C. Møller et M.S. Plesset, Phys. Rev. 46 (1934) 618–622.

[60] (a) P. Hohenberg, W. Kohn, Phys. Rev. B, 136 (1964) 864–871 (b) W. Kohn, L.J. Sham, Phys. Rev. A, 140 (1965) 1133–1138.

[61] W. Koch, M.C. Holthausen, A Chemist's Guide to Density Functional Theory, Wiley-VCH, Weinheim, 2000.

[62] A.D. Becke, J. Chem. Phys. 98 (1993) 5648–5652.

[63] C. Lee, W. Yang, and R. G. Parr, Phys. Rev. B, Condens. Matter. 37 (1988) 785–789.

[64] Y. Zhao and D. G. Truhlar, Theor. Chem. Acc., 120 (2008) 215-241.

[65] K.B. Wiberg, J. Comput. Chem. 25 (2004) 1342–1346.

[66] J. Tomasi, B. Mennucci, R. Cammi, Chem. Rev. 105 (2005) 2999–3094.

[67] B. Mennucci, R. Cammi, Continuum Solvation Models in Chemical Physics, Wiley-Blackwell, 2007.

[68] A.E. Reed, F. Weinhold, J. Chem. Phys. 78 (1983) 4066–4073.

[69] A.E. Reed, F. Weinhold, L.A. Curtiss, D.J. Pochatko, J. Chem. Phys. 84 (1986) 5687–5705.

[70] J. Cioslowski, J. Am. Chem. Soc. 111 (1989) 8333–8336.

[71] J. Cioslowski, Phys. Rev. Lett. 62 (1989) 1469–1471.

[72] M.J. Frisch, et al. Gaussian16, Revision B.01, Gaussian Inc., Wallingford CT, 2016.

[73] R. Dennington II, T. Keith, and J. Millam, GaussView, Version 4.1.2, Semichem Inc., Shawnee Mission, KS, 2007.

[74] Chem Office 8.0, CambridgeSoft.Com, Cambridge, M.A., USA, 2008.

[75] J. Elguero, C. Marzin, A.R. Katritzky et P. Linda, The Tautomerism of heterocycles, Academic Press, London, 1976.

[76] B. Mennucci, WIREs Comput. Mol. Sci. 2 (2012) 386–404.

[77] R. Cammi, Molecular Response Functions for the Polarizable Continuum Model, Springer International Publishing, New York, 2013.

[78] A. Ladjarafi, H. Meghezzi, Turkish Comp. Theo. Chem. (TC&TC) 2 (2018) 31–37.

[79] M. Caricato, Int. J. Quantum. Chem. 2019, 119, e25674.

[80] K.B. Wiberg, Tetrahedron 24 (1966) 1083–1096.

[81] M. Kowczyk-Sadowy, R. Świsłocka, H. Lewandowska, J. Piekut and W. Lewandowski, Molecules 20 (2015) 3146-3169.

[82] M. Cho, N. Sylvetsky, S. Eshafi, G. Santra, I. Efremenko, and J. M. L. Martin, Chemphyschem 21 (2020) 688–696.